An Experimental Study on Mechanical and Fracture Behavior of Phosphoric Iron

A. K. Vishnoi[a*], B.K. Mishra[a], S. Prakash[b]

[a] Department of Mechanical and Industrial Engineering, IIT Roorkee, India
[b] Department of Metallurgical and Materials Engineering, IIT Roorkee, India

*Corresponding Author: amitvishnoi.iitr@gmail.com

ABSTRACT

Phosphoric iron of two different phosphorus content, namely P_1 (Fe-0.30P-0.226C), P_2 (Fe-0.11P-.028C) were first prepared by ingot casting route. The ingot were soaked and forged at $1150^o C$. The microstructures of the phosphoric iron and its relevant mechanical properties such as hardness and tensile properties have been characterized. J-R curves of the material have been determined at room temperature. Fracture behaviour under tearing load has been studied through fracture toughness tests on phosphoric iron using Compact Tension (CT) specimens of Width (W) =50 mm and thickness (B) =12.5mm. J-R curves were obtained from specimens pre-cracked to a/W = 0.5 .The single specimen unloading compliance method have been used for generating J-R curves.

1. INTRODUCTION

Simple fracture is the separation of body into two pieces in response to the applied stresses. The applied stresses may be tensile, compressive, shear or torsional or a combination of them. Fracture of engineering structures is one of the most dreadful failures of the structural materials as it involves human lives and the structures itself. The problem of fracture has been greatly increased due to the amplified use of complex structures. As a result, extensive investigation were initiated in many countries and the work revealed that pre-existing flaws or high stress concentration region present in structure could initiate the crack and the propagation of such crack lead to the final fracture of the component or structure.

The corrosion behaviour of iron containing high phosphorous or phosphoric irons is an unexplored area of corrosion science and engineering. Recent research work on Delhi Iron Pillar [1-4], a good example of high phosphorus containing iron, has revealed some of its corrosion resistance properties. Research on Delhi Iron Pillar (DIP) provided the current impetus to

understand the corrosion behaviour of Fe-P alloy. The average composition of phosphorous in the DIP is about 0.25 wt%, while that of carbon is 0.15 % [2]. Irons, containing phosphorous contents of this order have been subjected to research by Balasubrahmaniyam et al [5]. His group has studied the corrosion properties of phosphoric iron manufactured by the ingot route [5].

Phosphorus increases the yield and ultimate tensile strengths with a corresponding reduction in ductility as measured by elongation and reduction in area, to a point where brittle failure occurs. This loss of ductility occurs during prolonged exposure of steel in the temperature range of 250-600^{0}C [6-9]. This condition is frequently encountered in tempering of steel. Hence it is called temper embrittlement. Phosphorous increases the ductile to brittle transition temperature of steel. It causes brittleness in steel during cold working [10-12].

In present work, an attempt has been made to determine the mechanical properties and fracture behaviour of phosphoric iron for two different phosphorus content, namely P_1 (Fe-0.30P-0.226C), P_2 (Fe-0.11P-.028C).

2. EXPERIMENTAL PROCEDURE

2.1 Materials

The materials used for the present investigation are the two compositions of phosphoric iron. The phosphoric irons were produced by ingot casting. For obtaining 1 kg of phosphoric iron containing 0.1 % P, we require 0.001 kg P. For obtaining 50 kg phosphoric iron with 0.1 % P, we require 0.050 kg P = 50 gm P. As 0.176 kg P is present in 1 kg Fe-P alloy, 0.050 kg P is present in 0.050/0.176 = 284 gm Fe-P = 0.284 kg of Ferro-phosphorous alloy. Similarly, for obtaining 0.3 % P, we require 0.003 kg P. For obtaining 50 kg phosphoric iron with 0.3 % P, we require 0.150 kg P = 150 gm P. As 0.176 kg P is present in 1 kg Fe-P alloy, 0.150 kg P is present in 0.150/0.176 = 852 gm Fe-P = 0.852 kg of ferro-phosphorous alloy.

2.1.1 Melting and casting

Utilizing a high frequency induction-melting furnace of 300 Kg capacity, 100 Kg of soft iron was first melted. To the molten iron, initially 25 Kg of steel scrap was added. During melting, slag covered the melt. Some of this slag was removed from the top of the melt. After proper melting of soft iron and steel scrap, approximately one third of the meet was transferred to a ladle, which was in the form of bucket of about 1.5 feet height. As per the calculations, the required amount of Fe-P mother alloy was added during taping of the melt into the ladle. Finally, the melt from the ladle was poured from the top side into a square mould, 50 cm height and 100cm square cross-section.

2.1.2 Reheating and soaking

A high temperature furnace was used for reheating the ingots and soaking at desired temperature (1150^{0}C). The ingots were placed in the furnace and the furnace was then heated. It took about 5

hours to reach the temperature (1150^0C). Ingots of different compositions were soaked at 1150^0C, successively for two hours of soaking. The logic for selecting 1150^oC is as follows. Heat- treating at this temperature is expected to produces a duplex microstructure consisting of austenite in the grain boundaries of ferrite.

2.1.3 Forging

Each ingot was forged at 1150^0C in to 25 mm thick plates. In successive stages of forging, each reduced plate was reheated again to 1150^0C for a short time for the further reduction of dimension. For example, when the thickness was reduced down to around 40 mm, the reduced plate is again reheated at 1150^0C for 15 minutes in the furnace for reheating purpose because longer time of reheating may lead grain growth. The 40 mm thick plate was again forged to obtain 25 mm thickness.

Table 1: Average composition of phosphoric iron after soaking and forging

| Sam Ple	C	P	Si	Mn	S	Ni	Cr	Mo	V	Cu
P_1	0.226	0.30	0.159	0.223	0.009	0.026	0.145	0.005	0.001	0.031
P_2	0.028	0.11	0.029	0.046	0.017	0.026	0.044	0.004	0.003	0.033

2.2 Hardness Evaluation

Hardness was evaluated with the help of a Vickers Hardness Tester using a load of 10 kgf. The specimen surfaces used for hardness studies were polished prior to hardness examination. At least five indentations were taken to estimate the average value of hardness of the phosphoric iron under investigation.

2.3 Tensile Testing

Round specimens of diameter 4mm and gauge length 16mm were fabricated for tensile tests following the ASTM standard E8 [13] from the as received block . The nominal dimensions of the tensile specimens are shown in **Fig. 1**. Specimens were fabricated for evaluating tensile properties. All tests were carried out at a cross-head velocity of 0.003 mm/sec. The tests were conducted at room temperature. The tensile data were analyzed to estimate the yield strength (YS), ultimate tensile strength (UTS), uniform elongation (eu), total elongation (et) and reduction in area.

Standard cylindrical tensile specimen according to ASTM E-8 used for tensile testing. Length of reduced section (A) is 20 mm, distance between shoulders (B) is 28 mm, diameter of reduced section (D_1) is 4 mm, grip diameter (D_2) is 8 mm, and radius of curvature (R) is 4mm.
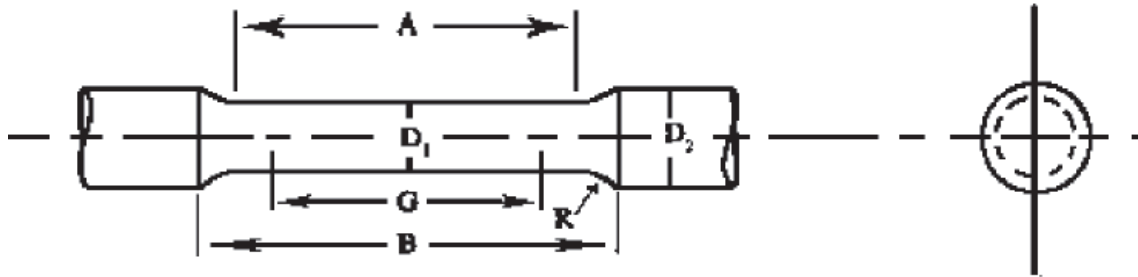
Figure 1: Nominal dimensions of the tensile specimens

2.4 J-Integral Test

2.4.1 Specimen preparation

The fracture toughness tests in this investigation were planned on compact tension specimens in L-T orientation. Considering the available form of the material, standard CT specimens were machined following the guidelines of ASTM E 399-90 [14], in orientation, LT of the crack plane. Typical configuration of a specimen is shown in **Fig. 2** the designed dimensions of the specimens were; thickness (B) = 12.5mm, width (W) = 50mm and machine notch length (a_N) = 10mm.
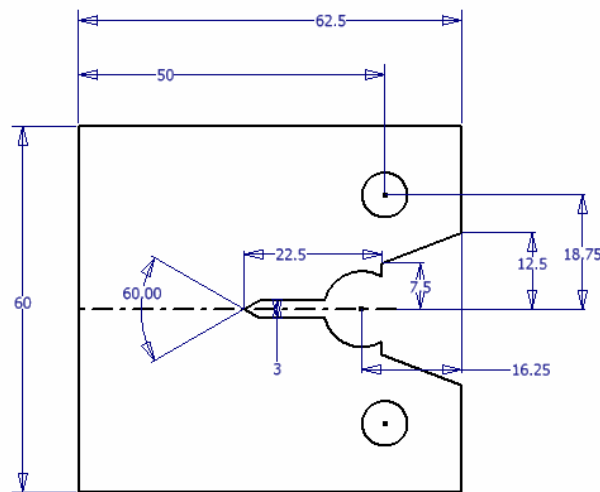
Figure 2: Dimensions of CT specimen

2.4.2 Fatigue pre-cracking

Testing was done at room temperature at cyclic stress frequency of 10 Hz. In the test fatigue crack was initiated and propagated under tension sinusoidal loading for a stress ratio R = 0.1, pre-cracking load calculated by the following formula

$$P_L = \frac{B b^2 \sigma_Y}{2W + a}$$

Where   B = thickness of CT specimen, σ_Y is yield strength, a initial crack length, b uncrack ligament, W = width of CT specimen.

For pre-cracking load condition is 0.4 P_L, P_{max}, P_{min} are calculated for pre-cracking of specimen

$$P_{max} = 0.4\ P_L$$
$$P_{min} = 0.1\ P_{max}\ (\text{stress ratio } 0.1)$$

2.4.3 Fracture toughness testing

In the single specimen J-integral tests unloading should not exceed more than 50% of the current load value and hence design and control of the test procedure is important. Some initial trial experiments indicated that a specific actuator displacement control for the selected iron could lead to the desired test procedure. This control consisted of loading a specimen to a level of 0.3mm, unloading through 0.15mm, reloading through 0.15mm and then repeating the sequence till an appreciable load drop was noticed on the load displacement plot. The displacement cycles were carried out using an actuator rate of 0.003 mm s^{-1}. The tests were controlled through a computer attached to the machine. The actuator displacement, load and the load line displacement (LLD), were recorded continuously throughout the test at a frequency of 2 Hz. The magnitude of LLD was monitored by a crack opening displacement (COD) gauge of 10 mm gauge length attached to the specimen. A minimum of approximately 35 data points of load-LLD was collected from the unloading part of the loading sequence for crack length calculations.

2.4.4 Generation of J-R curve:

Calculation of J: The magnitude of J is the sum of its elastic and plastic component denoted by J_{el} and J_{pl}. The elastic component of J was calculated using the equation

$$J = J_{el} + J_{pl}$$

$$J_{el} = K_i^2\ (1\text{-}v^2)\ /\ E + J_{pl}$$

where K_i the elastic stress intensity parameter is evaluated using the expression given below [15]

$$K_Q = \frac{P_i}{\sqrt{BB_n}\sqrt{W}} f\left(\frac{a_i}{W}\right)$$

$$f\left(\frac{a_i}{W}\right) = \left(2 + \frac{a_i}{W}\right)\frac{\left[.866 + 4.64\frac{a_i}{W} - 13.32\left(\frac{a_i}{W}\right)^2 + 14.72\left(\frac{a_i}{W}\right)^3 - 5.6\left(\frac{a_i}{W}\right)^4\right]}{\left(1 - \frac{a_i}{W}\right)^{3/2}}$$

The magnitude J_{pl} of was calculated by considering only load vs. plastic load line displacement. In order to obtain the latter, the elastic part of displacement at different loads was first calculated from the slope of the initial load-LLD diagram. A simple subtraction of the elastic component from the total displacement yielded the plastic part of LLD. The area under the load vs. plastic LLD data from the start of the test to the load of interest was calculated to obtain the magnitude of .This was done by using the expression [16]

$$J_{pl(i)} = \left[J_{pl(i-1)} + \left[\left(\frac{\eta_{(i-1)}}{b_{(i-1)}}\right)\frac{A_{pl(i)} - A_{pl(i-1)}}{B}\right]\left[1 - \gamma_{(i-1)}\frac{a_{(i)} - a_{(i-1)}}{b_{(i-1)}}\right]\right]$$

where ,

$$\eta_{(i-1)} = 2.0 + \frac{0.522 b_{(i-1)}}{W}$$

$$\gamma_{(i-1)} = 1.0 + 0.76b_{(i-1)}/W$$

The quantity $A_{pl(i)} - A_{pl(i-1)}$ is the increment of plastic area under the force versus plastic load-line displacement record between lines of constant displacement at points i-1 and i. The quantity $J_{pl(i)}$ represents the total crack growth corrected plastic J at point i and is obtained in two steps by first incrementing the existing $J_{pl(i-1)}$ and then by modifying the total accumulated result to account for the crack growth increment .Accurate evaluation of $J_{pl(i)}$ from the above relationship requires small and uniform crack growth increments consistent with the suggested elastic compliance spacing .The quantity $A_{pl(i)}$ can be calculated from the following equation.

$$A_{pl(i)} = A_{pl(i-1)} + \frac{1}{2}\left[(P_i + P_{(i-1)})(V_{pl(i)} - V_{pl(i-1)})\right]$$

where,
$V_{pl(i)}$ = plastic part of the load-line displacement, $V_{(i)} - (P_{(i)} C_{LL(i)},$ and
$C_{LL(i)}$ = experimental compliance, $(\Delta V/\Delta P)$, corresponding to current crack size

2.4.5 Calculation of crack size:

The inverse of the slope yielded the compliance (C_i) of the specimen corresponding to the load from which the unloading has been carried out. The obtained C_i –values were corrected for the

specimen rotation using the following expression to get the corrected compliance (C_{ci}) of the specimen at that particular load [17].

$$C_{ci} = \frac{C_i}{\left(\frac{H}{R}\sin\theta - \cos\theta\right)\left(\frac{D}{R}\sin\theta - \cos\theta\right)}$$

H = initial half-span of the load points (centre of pin holes)
R = radius of rotation of the crack centre line, (W + a)/2 where a is the updated crack length.
D = one half of the initial distance between the displacement measurement points
θ = angle of rotation of a rigid body element about the unbroken midsection line, or

$$\theta = \sin^{-1}\left[\frac{\frac{d_m}{2} + D}{(D^2 + R^2)^{\frac{1}{2}}}\right] - \tan^{-1} D/R$$

d_m = Total measured load-line displacement

The crack length (a_i) at this point of interest was next estimated using the expression suggested by Hudak et. al. [18]

$$\frac{a_i}{W} = 1.000196 - 4.0631u + 11.24u^2 - 106.043u^3 + 464.33u^4 - 650.677u^5$$

where,

$$u = \frac{1}{(BEC_{ci})^{1/2} + 1}$$

W = width of the specimen
B = total thickness of the specimen
The obtained values of J and the corresponding crack extension Δa were plotted to get the J- Δa curves of the material in various test conditions.

2.5 Fractography

The end of the ductile crack extension during loading of the specimens, subjected to J-integral test, was marked by post fatigue cracking, and then the specimens were loaded to fracture. The fractured surfaces were ultrasonically cleaned and examined using a scanning electron microscope. This was done to record the interesting features of stable crack extension.

3. Results and Discussions

Hardness was evaluated with the help of a Vickers Hardness Tester using a load of 10 kgf as shown in **Table: 2**. The five indentations were taken to estimate the average value of hardness of the steel under investigation.

**Table 2:** Hardness value of specimens

| SAMPLE	Hardness HV
P_{11}	202
P_{12}	190
P_{13}	210
P_{21}	179
P_{22}	170
P_{23}	165

3.1 Tensile Test

The tensile tests were conducted at room temperature. The stress strain plot for P_{11} and P_{12} is shown in **Fig. 3** while for P_{21} and P_{22} is shown in **Fig. 4** along with the tensile properties in **Table 3.**

Table 3: Tensile Properties of Phosphoric Iron P_1

Specimen	Yield stress, (MPa)	Ultimate tensile stress (Mpa)
P_{11}	434.7	664
P_{12}	344.2	573
P_{13}	480	610
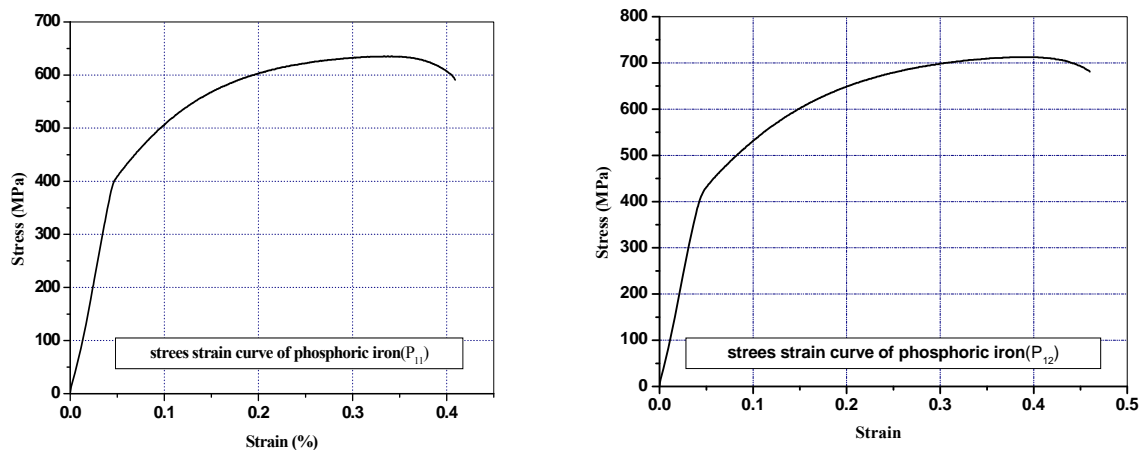
Figure 3: Stress strain diagram for specimen P_{11} and P_{12}
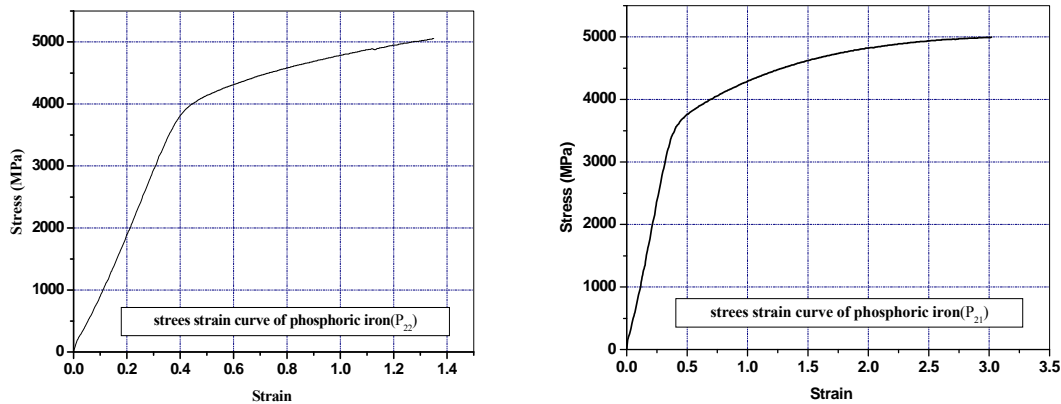
Figure 4: stress strain diagram for specimen P_{21} and P_{22}

3.2 J-integral Fracture Toughness

Pre-crack load was calculated as below:

$$P_{11max} = \frac{0.45b^2 \ \sigma_y}{2W+a} = 16.9 \ KN$$

$$P_{12max} = 11.53 \ KN$$

$$f\left(\frac{a_t}{W}\right) = \left(2+\frac{a_t}{W}\right)\frac{\left[.866 + 4.64\frac{a_t}{W} - 13.32\left(\frac{a_t}{W}\right)^2 + 14.72\left(\frac{a_t}{W}\right)^3 - 5.6\left(\frac{a_t}{W}\right)^4\right]}{\left(1-\frac{a_t}{W}\right)^{\frac{3}{2}}} = 8.34$$

Then an exclusion line is drawn parallel to the construction line intersecting the abscissa at 0.15 mm. A second exclusion line is drawn parallel to the construction line intersecting the abscissa at 1.5 mm. A J - Δa data points that fall inside the area enclosed by these two parallel lines are plotted.

In order to fit the power law equation for J-R curve, the experimental points of J vs. Δa lying between two exclusion lines were considered. The exclusion lines were constructed parallel to the experimental blunting line at Δa-offset values of 0.15 and 1.5mm following the ASTM standard E-1820 [37].

A line parallel to the experimental blunting line at Δa = 0.2mm was next constructed. The intersection of this offset line with the fitted J-R curve was considered as the critical value of J, i.e. J_Q.

A 0.2mm offset blunting line was drawn. The intersection of the blunting line with the power law curve at an offset of 0.2 mm was considered as J_Q. J_i was determined at intersection of blunting line with power law curve as shown in **Figure 5-8**.
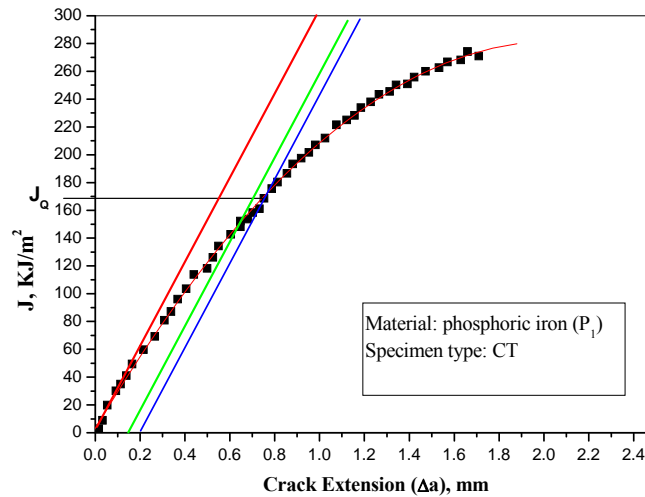
Figure 5 : J-R for curve specimen
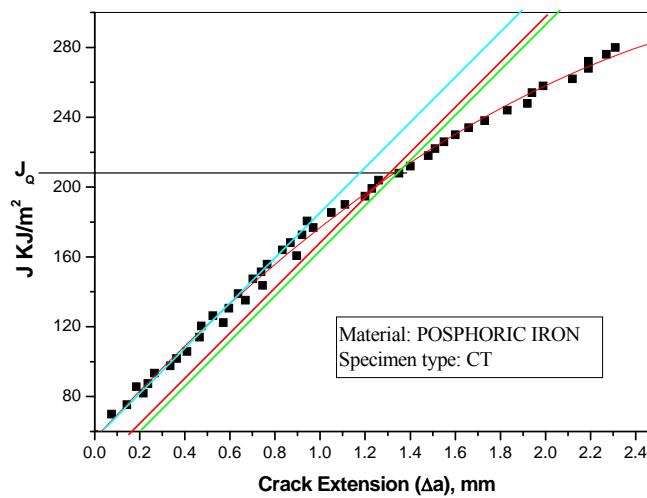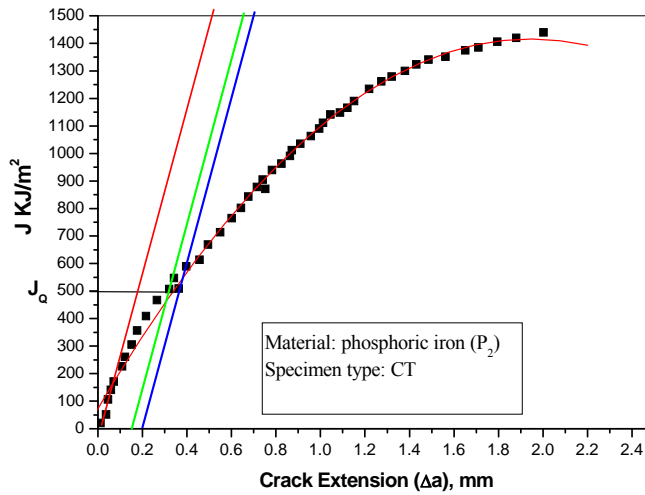

Figure 6: J-R for curve specimen P_{12}
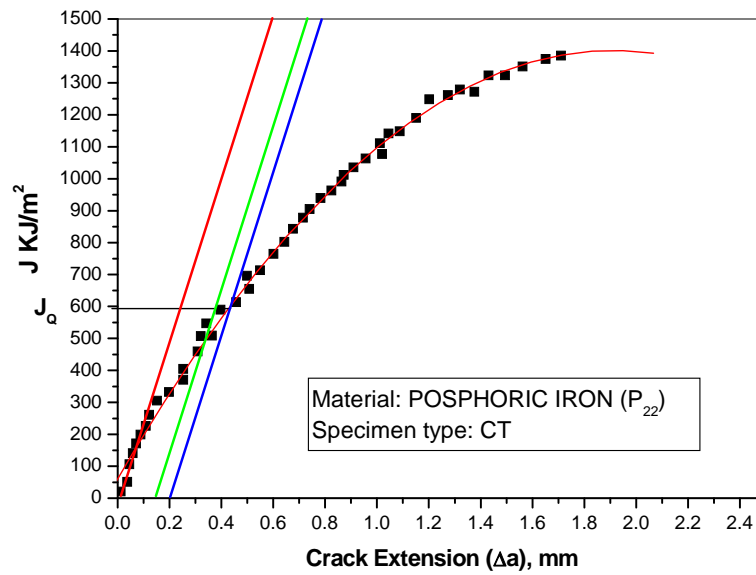
Figure 7: J-R for curve specimen P_{21}

Figure 8: J-R for curve specimen P_{22}

Table 4 : Thickness validity criteria of the specimens for fracture toughness test:

| Specimen	$\sigma_{o\ MPa}$	$J_{Q\ KJ/m^2}$	B	$10(J_Q/\sigma_o)$
P_{11}	549	170	12.5	3.0
P_{12}	458	210	12.5	4.5
P_{21}	376.4	500	12.5	13.3
P_{22}	371.1	590	12.5	15.8

σ_o = flow stress, J_Q = critical value of J
B = specimen thickness, and $10(J_Q/\sigma_o)$ = thickness criterion.

3.3 J Integral Fracture Toughness of Phosphoric Iron

The estimated average J-integral fracture toughness values of the phosphoric iron at room temperature are 170 KJ/m^2 (**Table 4**) for specimens P_{11}. And for specimen P_{12} is 210 KJ/m^2. J integral fracture toughness for P_{21} is 500 KJ/m^2. P_{21} and P_{22} specimen is fail in thickness criteria.

3.4 Fractography

The fractured surfaces were ultrasonically cleaned and examined using a scanning electron microscope. For P_1 specimen:

(a)   (b)
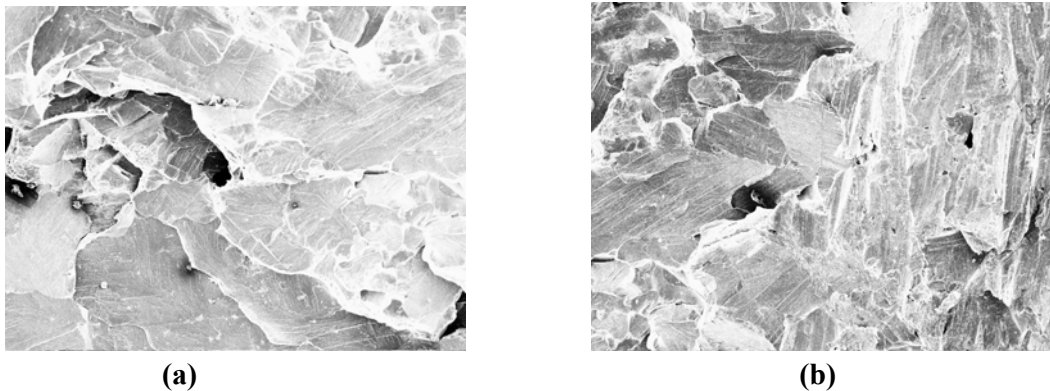
Figure 9 : SEM micrograph of fracture surface of specimen P_1 obtained at different magnification

(a)   (b)
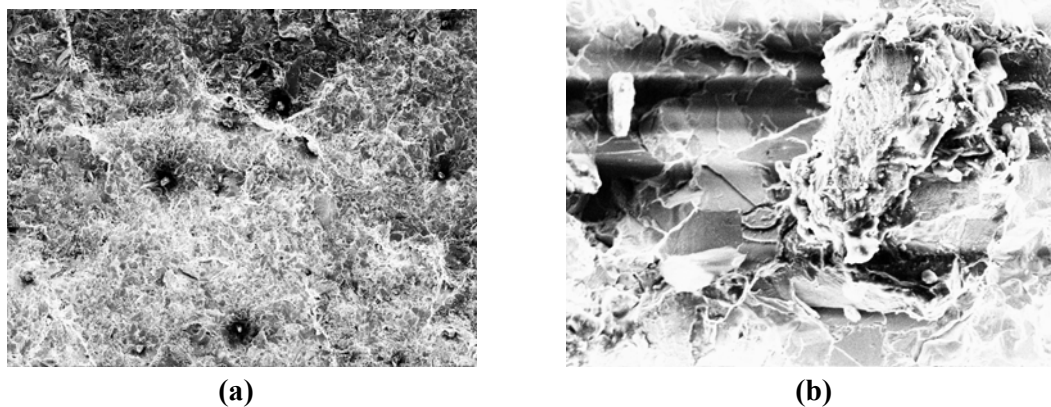
Figure 10: SEM micrograph of fracture surface of specimen P_2 obtained at different magnification

The fracture surface of specimen decohesive P_1(**Figure 9**) rupture (which is also called as inter-granular fracture) and brittle trans-granular cleavage fracture. Fracture surface of specimen as

received P_2 revealed equiaxed and elliptical dimple (**Figure 10**) under SEM which show the ductile behaviour.

4. CONCLUSION

The phosphoric iron P_1 (Fe-0.30P-0.226C), P_2 (Fe-0.11P-.028C) were prepared by ingot casting route. The ingots were soaked and forged at 1150 ^{0}C. The microstructures were subjected to metallographic examination. Mechanical properties and J_{IC} were evaluated and compare with mild steel.

Hardness of as received phosphoric iron increased with increasing phosphorus content, indicative of solid solution strengthening effect of phosphorus in phosphoric irons. Effect of phosphorus in phosphoric iron was confirmed from the observed increasing trend of yield stress and ultimate tensile stress with increasing phosphorus content. A decreasing trend of ductility (both percentage elongation and percentage reduction in area at failure) with increasing phosphorus content was also noted. The J_Q fracture toughness value of CT of P_1 specimen prepared from the phosphoric iron satisfy the criteria suggested in ASTM E- 1820 standard. Fracture toughness for specimen P_1 (Fe-0.30P-0.226C) is 170 KJ/m^2 and 210 KJ/m^2 It is comparable to mild steel (179KJ/m^2). Fracture surface of specimen as received P_2 revealed equiaxed and elliptical dimple under SEM, while that of P_1 (Fe-0.30P-0.226C) revealed both decohesive rupture and transgranular cleavage fracture. Phosphoric iron is a new class of engineering materials with good fracture toughness and corrosion resistance properties.

REFERENCES

1. R. Balasubrahmaniam, "On the Corrosion Resistance of the Delhi Iron Pillar". Corrosion Science, 42(2000), Pp: 2103-2129.
2. G Wranglen, "The Rustless Iron Pillar at Delhi". Corrosion Science, 10(1970),Pp: 761-770
3. R. balasubrahmaniam and AV Kumar." Characterization of the DIP Rust by XRD, FTIR and Mossbauer Spectroscopy". Corrosion science, 42(2000), Pp: 2085-2101
4. Gadadhar Sahoo and R. Balasubramaniam. " Corrosion of Phosphoric Irons in Acidic Enviornments" Journal of ASTM International, 5(2008), Pp: 1-7
5. R Balasubrahmaniam and A V Kumar, "On the Origin of High P Content in Ancient Indian Irons." International Journal of Metals, materials and processes, 14(2002), Pp: 1-14.
6. J M Capus and G Meyer, "The Mechanical Properties of Some Tempered Alloy Martensites". Journal of the iron and steel institute, 196(1960), Pp: 149-158.
7. C.L. Briant and S.K.Banerji, "Phosphorus Induced 350 ^{0}C Embrittlement in an Ultrahigh-Strength Steel", Metallurgical Transaction A: Physical Metallurgy and Materials Scince, 10 A (1979) 123-126.
8. R.M. Horn and R.O. Ritchie, "mechanism of tempered martensite embrittlement in low alloy steel," Metallurgical Transaction A: Physical Metallurgy And Materials Scince, 9 A (1978) 1039-1053

9.   J.P. materkowski and G. Krauss. "Tempered Martensite Embrittlement In SAE 4340 Steel". Metallurgical Transaction A : Physical Metallurgy And Materials Scince 10A (1979) 1643-1651

10. C.J. Mcmahon Jr., American Socity Of Testing Materials, ASTM STP 407 (1968) 127.

11. Y.Q. Weng and C.J.Mchmanhon, "Interaction Of Phosphorus, Carbon, Manganese, And Chromium In Intergranular Embrittlement Of Iron", Materials Science Technology, 3 (1987),207-216

12. M. Goodway and R.M. Fisher, "Phosphorus In Low Carbon Iron: Its Beneficial Properties", Historical Metallurgy, 22 (1988) 21-23

13. ASTM E 8M-94a, "Test Methods for Tension Testing of Metallic Materials (Metric)", Annual Book of ASTM Standards, Vol.03.01, p.81-100, ASTM, Philadelphia, PA, (1994)

14. ASTM E399, "Standard Test Method for Plan Strain Fracture Toughness of Metallic Materials", Annual Book of ASTM Standards, Section 3, (1996)

15. H. Roy, S. Sivaprasad, S. Tarafder, K.K. Ray, "Monotonic vis-à-vis cyclic fracture behavior of AISI 304LN stainless steel", Engineering Fracture Mechanics (2009)

16. ASTM E1820-08a Standard test method for Measurement of Fracture Toughness, Annual Book of ASTM Standards, Vol.03.01, p.1-34, ASTM, Philadelphia, PA, 2008

17. ASTM E 647-93, Standard Test Method for Measurement of Fatigue Crack Growth Rates, Annual Book of ASTM Standards, 1994, Vol.03.01, pp.569-596, ASTM, Philadelphia, PA.

18. Pickering F.B., [1977], "The structure and properties of banite in steels, in transformation and hardenability in Steels", Climax Molybdenum Company of Michigan, Ann Arbor, MI, p 109-13